JUNOCAM AT GANYMEDE: TOPOGRAPHIC MAPPING OF CRATERS, CALDERAS AND DOMES.

P. Schenk[1], G. C. Collins[2], C. J. Hansen[3], M. A. Ravine[4], and W.B. McKinnon[5]. [1]Lunar & Planetary Institute/USRA, Houston TX (schenk@lpi.usra.edu), [2]Wheaton College, Norton MA, [3]Planetary Science Institute, Tucson AZ, [4]Malin Space Science Systems, San Diego CA. [5]Washington University in St. Louis, Saint Louis MO 63130.

Introduction: On 7 June, 2021, Juno completed the first and only close spacecraft encounter with Ganymede between Galileo and the mapping missions of Europa Clipper and JUICE. JunoCam acquired 1-2.5 km pixel scale imaging of the northern subJovian hemisphere [1,2], improving our understanding of geologic features [3] in those regions poorly illuminated in earlier missions, but also acquiring low-Sun and stereoscopic imaging for topographic analysis in areas poorly covered by existing imagery [4]. Here we focus on topographic analysis of large-scale topography, craters and paterae (caldera-like features).

Topographic Mapping with JunoCam: With the release of JunoCam Ganymede data to the PDS it is now possible to apply ISIS mapping tools to register the 4 JunoCam scans [2] for DEM generation. The scans range from ~1 to 2 km/pixel and overlap sufficiently to produce a contiguous DEM over an area of ~9 million km^2 from ~30°W to 30°E and from ~10°S to 60°N, with vertical precisions of several hundred meters, sufficient to resolve the deeper craters (with depths of 500-1000 m) but not most geologic structures, which Voyager and Galileo stereo DEMs show to be a few hundred meters in amplitude [4]. Supplementing the stereo is shape-from-shading (PC-DEMs) which resolves geologic features such as craters, grooves, furrows, and paterae (caldera-like features) at pixel scales in northern areas between ~315-345°E (Fig. 1).

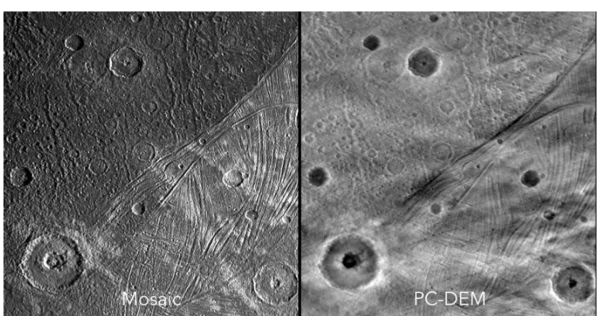

Figure 1. JunoCam mosaic (left) and preliminary PC-DEM (right) of southern Perrine Regio showing grooves, furrows, large central pit craters with domes, and both relaxed and unrelaxed craters. Scene is ~475 km across; DEM vertical scale is -750 to +750 m.

Craters: Several of Ganymede's major crater types are resolved in the stereo DEMs, including fresh central pit (e.g., Tros, D~92 km) and central dome craters, and anomalous dome craters (e.g, Neith) [5]. Tros, one of the most prominent rayed craters on Ganymede, is ~1 km deep with a ~1 km deep central pit but only a small offset central dome ~200 m high (Fig. 2a). Tros pit and crater depths, as well as several other large craters in mapping area, are consistent with previous VGR/GLL measurements of unmodified crater depths on Ganymede [6]. Although unusual, the small size of the central dome at Tros is also consistent with deep central pits and weak dome formation observed at a few other large craters such as Isis (D~72 km).

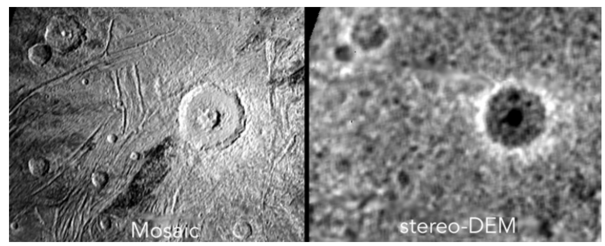

Figure 2a. JunoCam mosaic (left) & preliminary stereo-DEM (right) of 90-km-wide central pit Tros crater. DEM vertical scale -750 to +750 m.

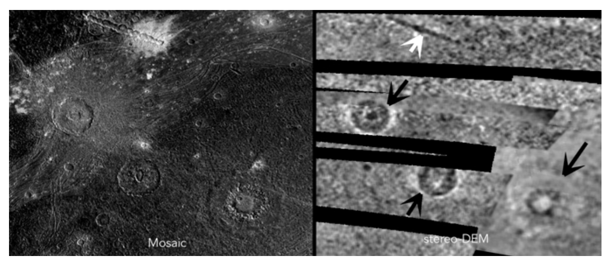

Figure 2b. JunoCam mosaic (left) and preliminary stereo-DEM (right) of southeastern Perrine Regio showing Enki Catena, prominent 90-km-wide craters and flattened 160-km-wide Neith anomalous dome crater at lower right. Scene is ~550 km across; DEM vertical scale is -750 to +750 m.

The JunoCam imaging stereo-DEM confirms a Galileo PC-DEM of anomalous dome crater Neith (Fig. 2b; [7]) showing it to be a highly flattened but slightly elevated structure with no rim scarp (relief of a few hundred m at most) but with a 400 m deep central pit and 800 m high central dome (relative to its base).

The JunoCam PC-DEM also shows numerous craters in relaxed and unrelaxed state and confirms that the spatial density of unrelaxed craters on bright and dark terrains are broadly similar indicating that both terrains have been accumulating craters in a low-heat flow regime since shortly after bright terrain formation [4]. A few tectonically modified craters are observed within bright terrain in these areas.

Paterae: Ganymede's caldera-like features [8], are semi-enclosed depressions with non-circular scallop-shaped raised rims (Fig. 3) that are always cross-cut by lanes of bright terrain. Approx. 18 of these structures were mapped in Voyager data [8]; our resurvey of the Galileo/Voyager (+Juno) global maps finds ~35 such structures, of which 8 are newly identified in the JunoCam images forming a loose cluster, with otherl ~10 poorly resolved provisional features. The JunoCam images and DEMs confirm that paterae are a few hundred meters deep and are associated with more recently formed lanes of bright terrain, some of which are smooth, others grooved (although resolution limits make characterization difficult in some areas). Paterae thus represent a late stage process in Ganymede's resurfacing [8, 9], although it is unknown whether they represent collapse, explosive or other processes.

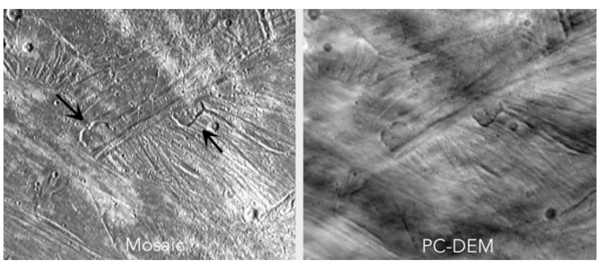

Figure 3. JunoCam mosaic (left) and preliminary PC-DEM (right) of Ganymede showing prominent 25-km-wide paterae (arrows) near 17°N, 327°E. Scene is ~250 km across; DEM vertical scale is -1000 to +1000 m.

Long-wavelength Topography: Although relief on Ganymede is very low (rarely exceeding +/- 1 km even in the larger fresh craters [4]) the possibility of topographic relief over length-scales of >100 km is suggested by possible gravity anomalies [10]. The identification of a 3-km-high dome (Fig. 4) at the sub-Jovian point [4] also indicates that Ganymede is capable today of supporting such relief, even if pervasive viscous relaxation [11] reduced such relief in the geologic record.

Fortuitously, JunoCam observed the subJovian dome in stereo, from which a DEM has been derived (Fig. 4). Previous measurements of the dome from a limb profile and serendipitous Voyager 1 stereo indicated a circular feature ~500 km across and 3 km high [4] but did not map the entire feature. The JunoCam stereo DEMs capture the entire feature and shows it to be ~475 by 700 km in size and oblong in the NE-SW direction. The JunoCam stereo coverage of Ganymede over much of the northern subJovian hemisphere (~9x10^6 km^2) found no additional domes. The presence of lower amplitude topographic distortions (related to internal mass [10]) remains unsettled as of this writing.

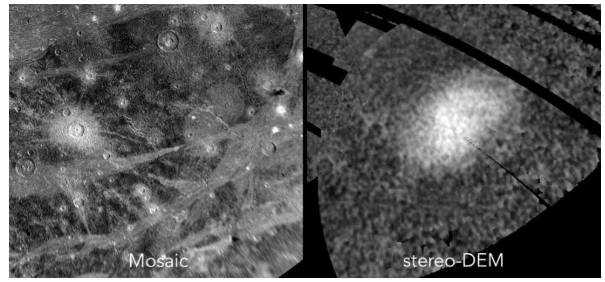

Figure 4. JunoCam mosaic (left) and preliminary stereo-DEM (right) of sub-Jovian point in Barnard Regio showing 450x750 km wide dome [4]. Scene ~1500 km across; DEM vertical scale -1000 to +3000 m. Any possible ring moat flanking the dome is as yet unconfirmed.

The new Juno constraints on the dome shape give a a total (above 0-km) volume of ~300,000 km^3 and a mass of ~3×10^{14} kg, assuming water ice (and twice this if there is an antipodal antiJovian dome). This is much smaller than the mass anomalies implied by the gravity signature [10]. The possibility that the G2 gravity anomalies may lie at depth, at Ganymede's ice-rock interface, could make the excess dome mass dynamically important to the orientation of the shell. Moreover, the dome may be the relaxed remnant of a much more massive and widespread crustal thickness anomaly, such as would be predicted to arise (in the absence of tidal heating) from the equator-to-pole temperature variation and which could in principle lead to TPW [12], moving thickened polar ice to the tidal axis [13]. Basal topographic compensation would eventually relax, but a shorter wavelength remnant at Ganymede's surface could in principle be preserved by the rigidity of cold surface ice late in geologic history under low heat flow.

Possible radial or concentric fractures which would reveal how the dome formed/evolved, detecting an antiJovian dome and mapping of Ganymede's internal mass distribution are questions that await future missions.

References: [1] Ravine, M. et al., (2021) *AGU*, abstract P42D-02. [2] Ravine, M. et al., (2022) *GRL*, to be submitted. [3] Collins, G., et al. (2022) this meeting. [4] Schenk, P. et al., (2022) in *Ganymede*, CUP. [5] Schenk, P., et al., (2004) in *Jupiter*, CUP. [6] Schenk, P. (2002) Nature, 417, 419-421. [7] White, O., et al., (2022) this meeting. [8] Schenk, P., and J. Moore (1995) *JGR*, 100, 19009-19022. [9] Head, J., et al., (1998) *LPSC* 29, #1666. [10] Palguta, J. et al., (2009) *Icarus*, 201, 615-625. [11] Bland, M. et al., (2017) *Icarus*, 296, 275-288. [12] Ojakangas G., and D. Stevenson (1989) *Icarus*, 81, 220-241. [13] McKinnon W.B. et al. (2014) *45th LPSC*, Abstract #1869.